Journal of Hazardous Materials 366 (2019) 703–713

Contents lists available at ScienceDirect

Journal of Hazardous Materials

journal homepage: www.elsevier.com/locate/jhazmat

Toxicity-based toxicokinetic/toxicodynamic assessment for bioaccumulation of polystyrene microplastics in mice

Ying-Fei Yang, Chi-Yun Chen, Tien-Hsuan Lu, Chung-Min Liao*

Department of Bioenvironmental Systems Engineering, National Taiwan University, Taipei, 10617, Taiwan, ROC

GRAPHICAL ABSTRACT

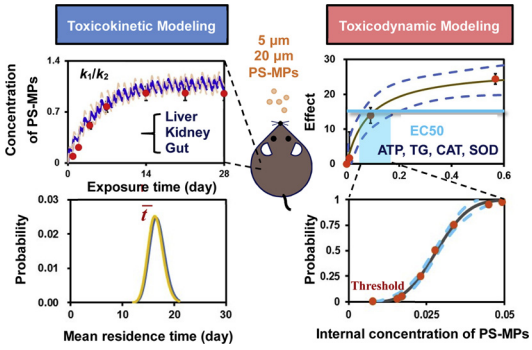

ARTICLE INFO

Keywords:
Microplastics
Polystyrene
Bioaccumulations
Toxicokinetic/ toxicodynamic
Mice

ABSTRACT

While a large body of literature has shown that microplastics (MPs) are highly likely to be accumulated in marine organisms and terrestrial animals, information about toxicity of MPs in mammal from a mechanistic point of view is more limited. Our paper fills this knowledge gap by assessing polystyrene (PS)-MPs-mice system based on toxicity-based toxicokinetic/toxicodynamic (TBTK/TD) modeling to quantify organ-bioaccumulation and biomarker responses appraised with published dataset. The key TBTK-parameters for mice liver, kidney, and gut posed by 5 or 20 μm PS-MPs could be obtained. We found that gut had the highest bioaccumulation factor (BCF) of ~8 exposed to 5 μm PS-MPs with a mean residence time of ~17 days. We showed that threshold concentrations of 5 and 20 μm PS-MPs among the most sensitive biomarkers were 8 ± 5 (mean ± SE) and 0.71 ± 0.14 μg g^{-1} bw, respectively, implicating that particle size was likely to affect TK/TD behavior in mice. The mice-based TK parameters and threshold criteria greatly assist in designing robust researches to evaluate MP consumption by humans. We establish a TBTK/TD framework for mechanistically assessing potential from mice size-specific MPs exposure that would offer a tool-kit for extrapolating to humans from health risk assessment perspective.

1. Introduction

Plastic debris is ubiquitous in both terrestrial and marine ecosystems due to the durability and indecomposable characteristics of plastics as discarded materials. Microplastics (MPs), defined as particles with diameter of at least one dimension < 5 mm, can occur as primary (e.g., cosmetic products or industrial abrasives) or secondary MPs from broken plastic debris caused by natural forces such as wave action,

* Corresponding author.
E-mail address: cmliao@ntu.edu.tw (C.-M. Liao).

https://doi.org/10.1016/j.jhazmat.2018.12.048
Received 12 September 2018; Received in revised form 28 November 2018; Accepted 14 December 2018
Available online 15 December 2018
0304-3894/

ultraviolet radiation, and hydrolysis [1–5]. In addition to the globally environmental threats of MP contamination, the issue of their potential toxicities to human health has recently raised serious concerns [6,7].

Scientific evidence for heightened pollution from MPs is mounting, yet appropriate administrative strategies to reduce human health risks posed by MP toxicities are lagging behind. It was reported that humans are potentially susceptible to MP toxicities due to the presence of MPs in frequently consumptive foods such as fish, shellfish, honey, sugar, and beer [8–15]. Several studies also revealed that commercial drinking and mineral water were contaminated with various types of microscopic plastic particles in high detected rates and unneglected amounts [16,17]. However, due to the limited knowledge of toxicology and biokinetics of MPs in mammals and human body, the mechanistic approaches based on present animal studies are necessitated to provide alternative methodologies for implementing human health risk assessment from MPs exposure.

Toxicity-based-toxicokinetic (TBTK)/toxicodynamic (TD) modeling is a powerful mechanistic approach elucidating fate and behaviors of specific pollutants, enabling to translate exposure to time course of toxic effects on related biomarkers [18–20]. TKs refers to concentrations of a toxicant change in time course encompassing absorption, distribution, biotransformation, and elimination of toxicants with application of mathematical descriptions. TDs deals with effects of a toxicant ranging from levels of molecular, cells, tissues, and organs to population leading from toxic actions to subsequent hazards and impairments in organisms. The TBTK/TD model can incorporate TK and TD processes by linking external exposure concentrations to biologically effective doses. Therefore, TBTK/TD modeling can be implemented as a rigorously quantitative framework to explore toxicity interactions of MPs in organisms.

Notably, information regarding MP toxicities in mammals are rarely explored. A pioneering polystyrene microplastic (PS-MP) study for mice was conducted by Deng et al. [21] with 5 and 20 μm fluorescent PS-MPs daily exposures resulted in accumulations of both sizes of particles in the liver, kidney, and gut. Also, alterations in metabolic profiles revealed PS-MPs impacts on energy and lipid metabolism, and oxidative stress in mice liver [21]. Polystyrene (PS) is one of the main polymer types in plastic products along with accompanied wastes in that PS-specific MPs are commonly found in MP fields [1,22,23]. PS-MPs are also widely applied in bioassays examining biological interactions and toxicities in organisms [2,24,25]. Given concerns for human health risks posed by MPs exposure, the TBTK/TD modeling constructed in this study can be assisted as a robust mechanistic tool to evaluate appropriate internal PS-MP concentrations in mice that are generally served as a mammalian terrestrial model organism.

Therefore, the purposes of this study were threefold: (1) to obtain TK parameters and dose-response profiles in mice posed by PS-MPs exposure appraised with the related published literature, (2) to quantify acceptable levels of PS-MPs in mice based on various biomarker responses to implicate threshold exposure doses, and (3) to provide an extrapolation tool along with the implemented methodologies for human health risk assessment.

2. Materials and methods

2.1. Study data

Experimental data related to bioaccumulations and toxic effects posed by exposures of PS-MPs in various dosages were adopted from Deng et al. [21] (Supplementary Tables S1 and S2). Briefly, the PS-MPs beads in size diameters of 5 and 20 μm were applied in both accumulation bioassays and toxicity treatments in five-week-old male mice *Mus musculus* as described in Fig. 1A [21]. Accumulation bioassays were conducted to determine distributions and accumulations of size-specific PS-MPs in liver, kidney, and gut of mice (Fig. 1B). Two groups with each of 35 mice were treated daily via oral gavage with 0.2 mg mL^{-1} fluorescent PS-MPs with sizes of 5 or 20 μm in water. Five mice were sacrificed at 1, 2, 4, 7, 14, 21, and 28 days post treatments.

Toxicological experiments were performed to analyze energy and lipid metabolisms and oxidative stress in mice liver (Fig. 1B) [21]. Except the control group, each group with five mice were treated with 5 or 20 μm PS-MPs in doses of 0.01, 0.1, and 0.5 mg day^{-1} for 4 weeks. Liver samples were removed post treatments to evaluate alterations of biomarkers of adenosine triphosphate (ATP), triglyceride (TG), catalase (CAT), and superoxide dismutase (SOD) in mice [21].

2.2. Exposure assessment

To rigorously estimate time-dependent internal concentrations of PS-MPs in mice based on the exposure scenarios of Deng et al. [21], the Dirac delta function was used to mathematically describe the sequential pulsed exposure patterns in accumulation bioassays [21]. The time-dependent exposure concentrations of 5 or 20 μm PS-MPs in mice can be written as,

$$C_w(t) = C_0 + C_1 \sum_n \delta(t - nT), \tag{1}$$

where $C_w(t)$ is the time-dependent PS-MPs concentration in water (mg mL^{-1}), t is the exposure time (day), C_0 is the environmental background concentration of PS-MPs (mg mL^{-1}), C_1 is the pulsed exposure concentration of PS-MPs at 0.2 mg mL^{-1}, δ is the Dirac delta function, n is the pulsed frequency during exposure, and T is the time between adjacent pulsed intervals (day).

2.3. TBTK modeling

The TBTK model is a first-order differential model dealing with the kinetic process of chemical-biota interactions (Fig. 1C). The time-dependent 5 or 20 μm PS-MPs concentrations in specific organs ($C_i(t)$) of mice can be predicted by the one-compartment TK model as,

$$\frac{dC_i(t)}{dt} = k_1 C_w(t) - k_2 C_i(t), \tag{2}$$

where $C_i(t)$ is the time-dependent PS-MPs concentrations in specific organ i (mg g^{-1} bw), k_1 is the uptake rate constant from the mixed solution of PS-MPs in mice (mL g^{-1} day^{-1}), k_2 is the depuration rate constant from PS-MPs in organs of mice (day^{-1}) (Fig. 1D).

Based on the experiment settings of Deng et al. [21], the dynamic internal concentrations of PS-MPs in mice posed by orally pulsed exposures of PS-MPs can be estimated by incorporating Eqs. (1) to (2), resulting in the unit step function (U) as,

$$C_i(t) = C_1 \cdot k_1 \cdot e^{k_2 - k_2 t} \sum_{n=1}^{28} e^{(n-1)k_2} U(-n + t), \tag{3}$$

In addition, when the PS-MPs-mice interaction reaches steady state with a saturation curve, the steady-state bioconcentration factor (BCF_{ss}) in specific organs of mice can be expressed as the TK parameters,

$$BCF_{ss} = \frac{C_i}{C_w} = \frac{k_1}{k_2}. \tag{4}$$

2.4. Mean residence time estimation of PS-MPs

The mean residence time (MRT) was determined based on the experimental data from accumulation assay performed by Deng et al. [21] (Fig. 1C; Supplementary Table S1). The size- or organ-specific MRT in PS-MPs-mice system can be estimated as,

$$\overline{t_i} = \frac{\int_0^t t C_i(t) dt}{\int_0^t C_i(t) dt}, \tag{5}$$

where $\overline{t_i}$ is the MRT of PS-MPs in a specific organ i (day) (Fig. 1D).

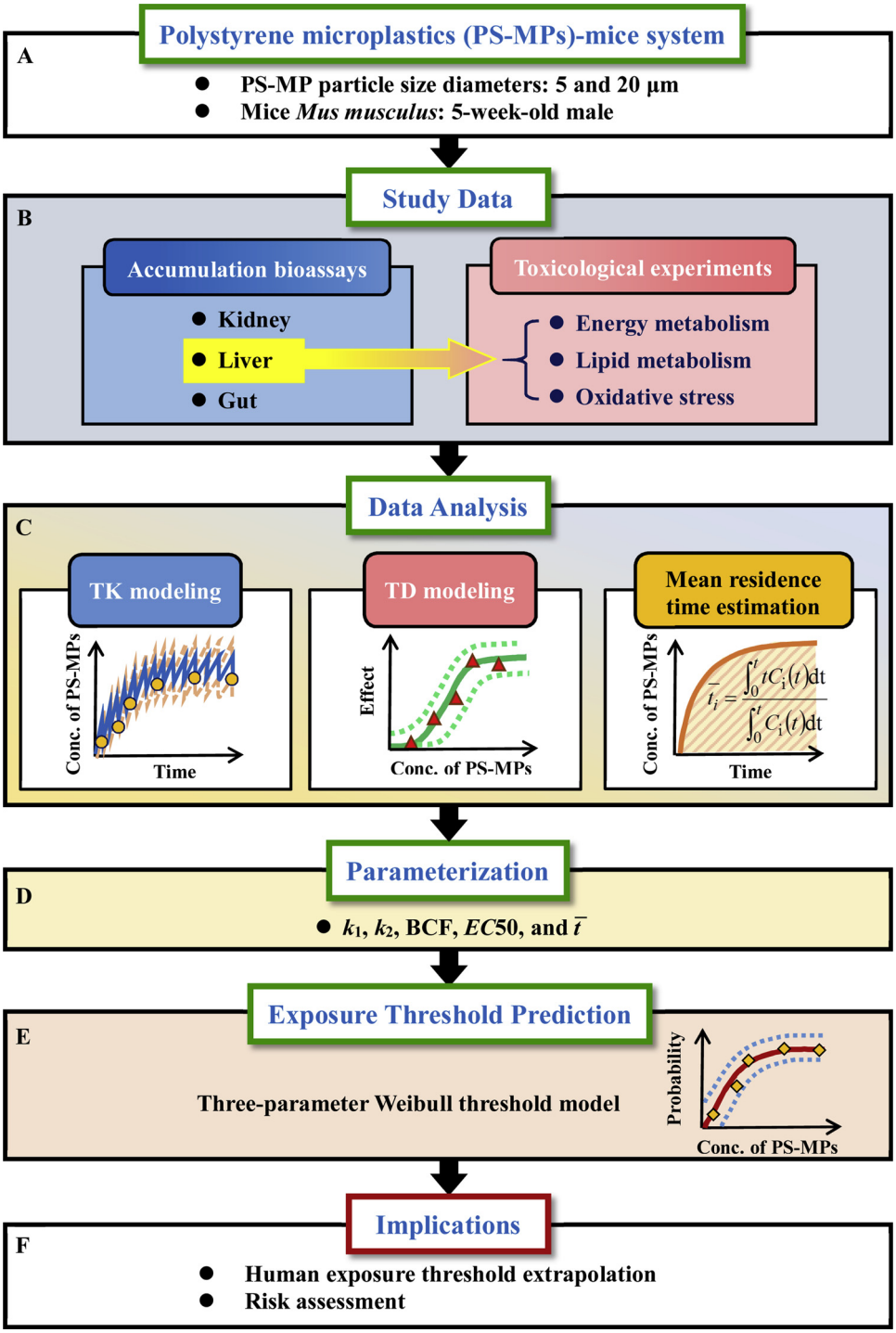

Fig. 1. Schematic showing the study framework and computational algorithm.

2.5. Dose-response based TD modeling

To construct the relationship between physiological responses and PS-MPs burdens in mice liver, the Hill model was adopted to fit the TD experimental data (Fig. 1C). PS-MPs burdens in mice liver posed by various exposure concentrations were converted by multiplying the estimated BCF_{ss} and divided by the liver weight ranging from 1.47 to 1.74 g as described by Deng et al. [21]. A three-parameter Hill-based TD model can be written as,

$$E(C_L) = \frac{E_{max} \times C_L^{n_H}}{EC50^{n_H} + C_L^{n_H}}, \quad (6)$$

where E is the alteration of biomarkers effect, including ATP, TG, CAT, and SOD in mice liver (%), C_L is the internal concentration of PS-MPs in mice liver (mg g^{-1} bw), E_{max} is the maximum effect (%), $EC50$ is the internal concentration of PS-MPs that causes the half of E_{max} (mg g^{-1} bw) (Fig. 1D), and n_H is the Hill coefficient representing the slope of the dose-response model.

2.6. Predictive risk threshold

Based on the different dose-response trends in mice, a three-parameter Weibull threshold model can be applied to fit the percentile

values of 2.5th, 5th, 25th, 50th, 75th, 95th, and 97.5th extracted from the cumulative density functions of *EC*50 with 95 percentile confidence interval (CI) values estimated in each biomarker (Fig. 1E). The predictive risk threshold model can be expressed as,

$$F(C_L) = 1 - \exp\left[-\left(\frac{C_L - \gamma}{\alpha}\right)^{\beta}\right],\ C_L > \gamma > 0,\ \alpha > 0,\ \beta > 0, \quad (7)$$

where $F(C_L)$ represents the cumulative probability of internal PS-MPs concentrations in liver, γ is the threshold value (mg g^{-1} bw), α is the scale parameter (–), and β is the shape parameter (–).

2.7. Extrapolation algorithm

The overall algorithm of extrapolation methodology from mice to human system was described based on the well-constructed guidelines of interspecies dose conversion by the US Food and Drug Administration [26]. Conversion of PS-MPs doses from mice to human equivalent doses (HEDs) could be derived based on the no-observed-adverse-effect-level (NOAEL) in mice, reference body weights of mice (W_{mice}) (0.02 kg) and human (W_{human}) (60 kg), and an allometric exponent (b) [27] as follows,

$$\text{HED} = \text{mice NOAEL} \times (W_{mice}/W_{human})^{(1-b)}. \quad (8)$$

Moreover, to estimate more rigorous standards for PS-MPs levels in human, the NOAEL of mice for HEDs estimations was replaced with threshold doses of each biomarker estimated from the Weibull threshold model. The HEDs values were furtherly divided by a historically accepted default safety factor of 10 to allow variabilities in extrapolating animal to human systems [27,28]. The safety factor is accountable for differences in biological and physiological processes and sensitivities to specific toxicants between mice and human systems [27,28].

2.8. Simulation tools and uncertainty analysis

This study employed the Table curve 2D (Version 5.01, AISN Software Inc., Mapleton, OR, USA) to simulate all model fittings to the published data. Ordinary differential equations (ODEs) in analysis of TBTK modeling were solved with the Mathematica® (Version 11.2, Wolfram Research Inc., Champaign, IL, USA). The Crystal Ball® software (Version 2000.2, Decisionerring, Inc., Denver, Colorado, USA) was employed to implement Monte Carlo (MC) simulation which can be performed 10000 iterations to sufficiently ensure the uncertainties of simulation results. Percentiles of 2.5th and 97.5th are generated as the 95% CIs for all model fittings.

3. Results

3.1. TBTK analysis of PS-MPs in mice system

TBTK-parameter estimates of k_1 and k_2 for mice liver, kidney, and gut posed by 5 or 20 μm PS-MPs exposure were obtained by fitting the first-order TK model (Eq. (2)) to exposure data (Fig. 2; Table 1; Supplementary Table S1). Overall, both estimated k_1 and k_2 values were the highest in gut with k_1 = 2.5 ± 0.2 mL g^{-1} d^{-1} (mean ± SE) and k_2 = 0.31 ± 0.03 d^{-1} for 5 μm, and k_1 = 1.5 ± 0.1 mL g^{-1} d^{-1} and k_2 = 0.33 ± 0.03 d^{-1} for 20 μm (Table 1). Specifically, the k_2 estimates for 5 μm PS-MPs in three organs were close to those of 20 μm (Table 1).

The BCF_{ss} values were the highest in gut, followed by kidney and liver with average estimates of 8.16, 5.57, and 1.59, respectively, for 5 μm PS-MPs, whereas the estimated BCF_{ss} values in the treatment of 20 μm PS-MPs were approximately the same among three organs ranging from 4.47 to 4.66 (Table 1).

3.2. MRT of PS-MPs in mice system

The MRTs of 5 or 20 μm PS-MPs were estimated (Fig. 3). Predicted MRT values in liver, kidney, and gut posed by 5 μm PS-MPs exposures were approximately the same with estimates of 16.74 (95% CI: 11.41–22.15), 17.12 (12.33–22.36), and 16.06 (11.85–20.74) days, respectively (Fig. 3A). Similarly, the estimated MRTs of 20 μm PS-MPs in liver, kidney, and gut were close to that of 5 μm with estimates of 16.28 (11.23–21.16), 17.02 (11.68–22.50), and 15.97 (12.18–20.37) days, respectively (Fig. 3A).

The MRTs in three organs posed by 5 μm PS-MPs exposure were estimated by fitting to a lognormal (LN) function with a geometric mean (gm) of 16.66 days and a geometric standard deviation (gsd) of 1.09, denoted as LN(16.66, 1.09) (Fig. 3B). Close to the estimated MRT ranges of 5 μm PS-MPs, the fitted result of 20 μm PS-MPs among three organs was LN(16.38, 1.09) (Fig. 3B).

3.3. TD analysis of PS-MPs in mice system

The dose-response relationships between internal burdens of PS-MPs and biomarker alteration in mice liver were well fitted to three-parameter Hill-based TD model (r^2 = 0.72 – 0.94; p-value < 0.05) (Fig. 4; Supplementary Tables S2 and S3). The E_{max} associated with 5 μm PS-MPs exposure for inhibited activities of ATP, TG, and CAT were 39 ± 4 (mean ± SE), 28 ± 5, and 22 ± 4%, respectively (Fig. 4A, C, E; Supplementary Table S3). Under 20 μm PS-MPs exposure, estimated E_{max} values for ATP, TG, and CAT inhibitions were 39 ± 4, 29 ± 4, and 27 ± 5%, respectively (Fig. 4B, D, F; Supplementary Table S3).

Increment of SOD activities posed by 5 and 20 μm PS-MPs exposures had average E_{max}s of 51.91 and 40.22%, respectively (Fig. 4G, H; Supplementary Table S3). Results also indicated that the internal concentrations of 5 μm PS-MPs given *EC*50 for ATP, TG, CAT, and SOD were 0.03 ± 0.01 (mean ± SE), 0.09 ± 0.05, 0.04 ± 0.02, and 0.05 ± 0.02 mg g^{-1} bw, respectively (Fig. 4A, C, E, G; Supplementary Table S3). For 20 μm PS-MPs, the *EC*50 of ATP activity inhibition showed similar results to that of 5 μm PS-MPs with estimate of 0.03 ± 0.01 mg g^{-1} bw (p-value < 0.05) (Fig. 4B, Supplementary Table S3).

TG and CAT inhibitions and SOD activity increment were all different compared to that of 5 μm PS-MPs treatments with estimates of 0.19 ± 0.09, 0.24 ± 0.12, and 0.02 ± 0.01 mg g^{-1} bw, respectively (Fig. 4D, F, H; Supplementary Table S3). The fitted n_H were larger than 1 in all dose-response fittings, indicating the positive cooperativity between PS-MPs and biological responses related to energy metabolism, lipid metabolism, and oxidative stress in mice liver (Supplementary Table S3).

3.4. Predictive risk threshold of PS-MPs

We utilized the results from TD analysis to further predict threshold concentrations of size-specific PS-MPs inducing biomarker alternations in mice. The extracted percentile data were significantly well fitted to the Weibull threshold model (r^2 > 0.96; p-value < 0.001) (Fig. 5; Supplementary Tables S4 and S5). The predicted thresholds causing 50% inhibition or increment of biomarkers in mice liver posed by 5 μm PS-MPs exposure are in the following order of TG > SOD > CAT > ATP with estimates of 40.02 ± 2.29 (mean ± SE), 12.61 ± 0.98, 10.57 ± 1.09, and 7.90 ± 4.57 μg g^{-1} bw, respectively (Fig. 5A, C, E, G; Supplementary Table S5).

Different from the threshold order of 5 μm PS-MPs, CAT inhibition has the highest threshold concentration in mice treated with 20 μm PS-MPs, followed by TG, ATP, and SOD alternations with estimates of 91.39 ± 5.38, 88.09 ± 4.73, 1.74 ± 3.92, and 0.71 ± 0.14 μg g^{-1} bw, respectively (Fig. 5B, D, F, H; Supplementary Table S5).

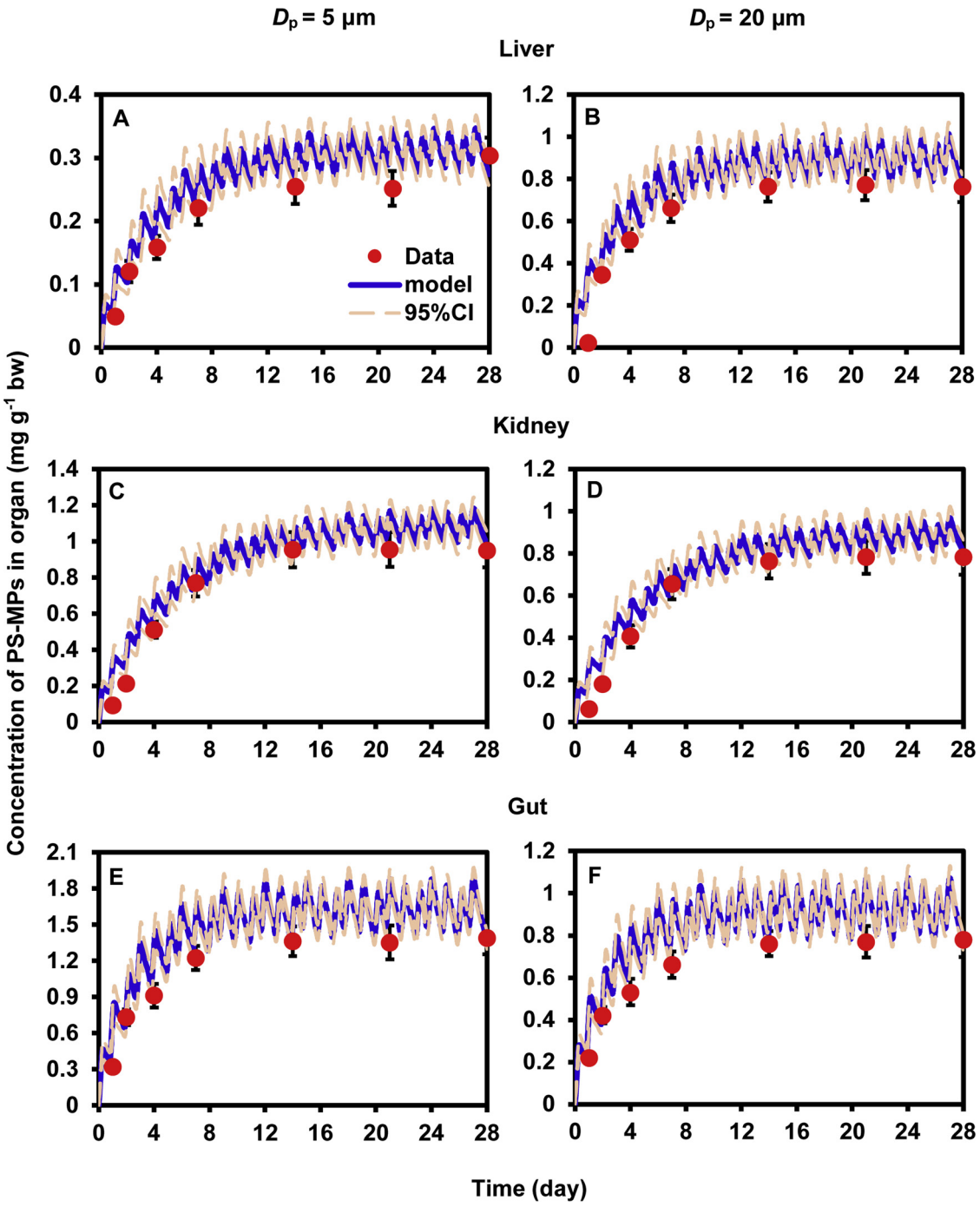

Fig. 2. Fitting of 28-d bioaccumulation experiments by a toxicokinetic model in (A, B) liver, (C, D) kidney, and (E, F) gut of mice exposed to 5 and 20 μm diameter of PS-MPs.

3.5. Proposed extrapolation method from mice to human system

A proposed extrapolation algorithm to estimate 5 or 20 μm PS-MPs threshold concentrations with biomarkers of energy and lipid metabolisms and oxidative stress in human was illustrated in Fig. 6. To derive HEDs with various biomarkers, threshold concentrations in mice should be firstly determined by applying the Weibull threshold model (Fig. 6A). Subsequently, an well-described empirical approach namely "dose by factor" could be adopted to estimate HEDs of 5 or 20 μm PS-MPs for various biomarkers based on estimates of mice threshold concentrations (Fig. 6B) [29]. The HEDs could be furtherly transformed into human doses by applying a safety factor with a value of 10 (Fig. 6C). In the risk assessment framework of human systems, k_1 and k_2 estimates derived from the TK/TD assessment could be adopted to estimate internal PS-MPs doses in mice if environmental concentrations of PS-MPs are available (Fig. 6D). Internal doses of PS-MPs in mice could be furtherly transformed into human doses by applying the extrapolation algorithm (Fig. 6D). To quantitatively characterize potential risks of PS-MPs in human body, risk quotients (RQs) could be derived by applying the transformed PS-MPs doses in human body and human threshold concentrations estimated in this study (Fig. 6D).

Table 1
The organ-specific estimated values of uptake rate constant (k_1), depuration rate constant (k_2), and steady-state bioconcentration factor (BCF_{ss}) in mice system posed by PS-MPs in particle diameter (D_p) = 5 and 20 μm.

k_1 (mL g^{-1} day^{-1})		k_2 (day^{-1})		BCF_{ss}	
D_p (μm)					
5	20	5	20	5	20
		Liver			
0.36[a]	1.19	0.23	0.27	1.59	4.47
(0.04)[b]	(0.13)	(0.03)	(0.03)	(0.26)	(0.68)
		Kidney			
0.99	0.82	0.18	0.18	5.57	4.60
(0.10)	(0.09)	(0.02)	(0.02)	(0.79)	(0.69)
		Gut			
2.50	1.52	0.31	0.33	8.16	4.66
(0.23)	(0.14)	(0.03)	(0.03)	(1.11)	(0.64)

[a] Mean.
[b] SE (p-value < 0.001).

4. Discussion

4.1. Bioaccumulation of MPs in various terrestrial organisms

Sources of MPs pollution in terrestrial regions especially for soil ecosystems are mainly from landfill of sewage sludge, discharge of municipal wastewater effluent, and plastic mulch applied in agricultural activities [30]. Compared to the growing evidence of MPs accumulations in marine system, limited parallel researches were observed in terrestrial systems due to difficulties in investigating accumulation patterns of MPs in the complex organo-mineral soil matrix [31]. Liu et al. [32] have reported the existence of MPs in farmlands of Shanghai with approximate abundances of 78 ± 13 and 63 ± 13 items kg^{-1} in shallow (0–3 cm) and deep (3–6 cm) soils, respectively, indicating the relatively lower accumulations of MPs in terrestrial region compared to marine system.

Based on the analysis of TBTK/TD modeling, we observed that different sizes of PS-MPs could influence bioaccumulations and biokinetic constants among terrestrial organisms. Particularly, uptake rate constant (k_2) and steady-state bioconcentration factor (BCF_{ss}) in each organ showed similar trends that treatments of smaller PS-MP size (5 μm) resulted in higher values, whereas the larger size (20 μm) exhibited lower values. Similarly, Besseling et al. [33] pointed that there were no MP particles accumulated in lugworms *Arenicola marina* while the uptake PS-MPs were in sizes of ≥ 400 μm [33]. Size-selective egestion was also observed in earthworms in that 90% of MPs were found in casts and small MP particles were preferentially retained in the worms [34].

However, it should be noted that the relatively low abundances of MPs in terrestrial environment reveal that significant tissue accumulations via direct assimilation in larger organisms were unlikely to be observed, whereas transfer across trophic levels or biomagnification along the food chain shows apparently plausible [35]. Huerta Lwanga et al. [34] suggested that bioaccumulation of MPs in earthworms *Lumbricus terrestris* could cause long-term ecological effects, leading to transfer of MPs to other terrestrial organisms due to the role as a base of many food chains.

A recent study also demonstrated transfer of MPs through terrestrial food chain in home gardens of Southeast Mexico, indicating that MPs concentrations were 0.87 ± 1.9 particles g^{-1} soil, 14.8 ± 28.8 particles g^{-1} casts, and 129.8 ± 82.3 particles g^{-1} chicken feces in soil, earthworm casts, and chicken feces, respectively [36]. Moreover, biomagnification factors between soil and earthworm casts and soil and chicken feces were found to be 17 ± 14.6 and of 149 ± 41.8, respectively [36]. It was also detected that the human consumption relevant food of chicken gizzards contained approximate 10.2 ± 13.8 M P particles [36].

Furthermore, MPs bioaccumulations in higher trophic levels of terrestrial ecosystems were explored in limited literature. Zhao et al. [37] demonstrated that the mean abundance of MPs in 17 terrestrial birds in Shanghai was 10.6 ± 6.4 particles per bird with higher MPs in stomach than in esophagus and intestine. Also, MPs concentrations did not vary significantly among three parts of stomach, esophagus, and intestine of the digestive tract, implying that the potentially toxic anthropogenic MPs were not immediately excreted from the digestive tracts. It was also indicated that longer retention of MPs could aggravate its potential to create physical and chemical damages to the ingestion abilities of wildlife [37].

4.2. Toxicity of MPs in terrestrial ecosystem

We have estimated threshold concentrations of PS-MPs based on dose-response profiles of biomarkers such as energy and lipid metabolisms and oxidative stress in mice. Except for the applied biomarkers in mice liver, significant elevation of neurotoxicity in terms of acetylcholinestrera (AChE) activity were evidenced [21]. Histological lesions including signs of inflammation and altered metabolomics were also observed in mice liver post PS-MPs treatments [21]. Lu et al. [38] observed significantly decrements of body, liver, and lipid weights in mice orally exposed to 1000 μg L^{-1} PS-MP with size of 0.5 or 50 μm for 5 weeks [38]. It was also demonstrated that orally-exposed MPs were capable of altering richness and diversity of gut microbiota, penetrating intestinal barrier, and being delivered into mice liver and kidney [21,38,39]. Furthermore, consistent in the biological responses adopted

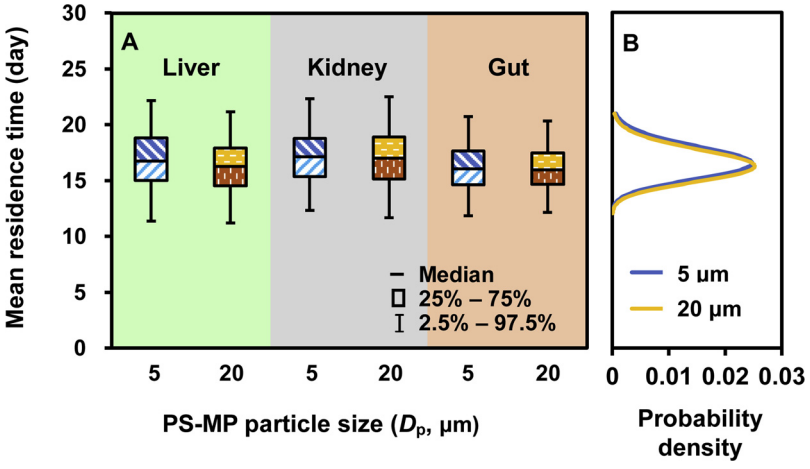

Fig. 3. (A) Organ-specific mean residence times and (B) probability densities of 5 and 20 μm MPs accumulations.

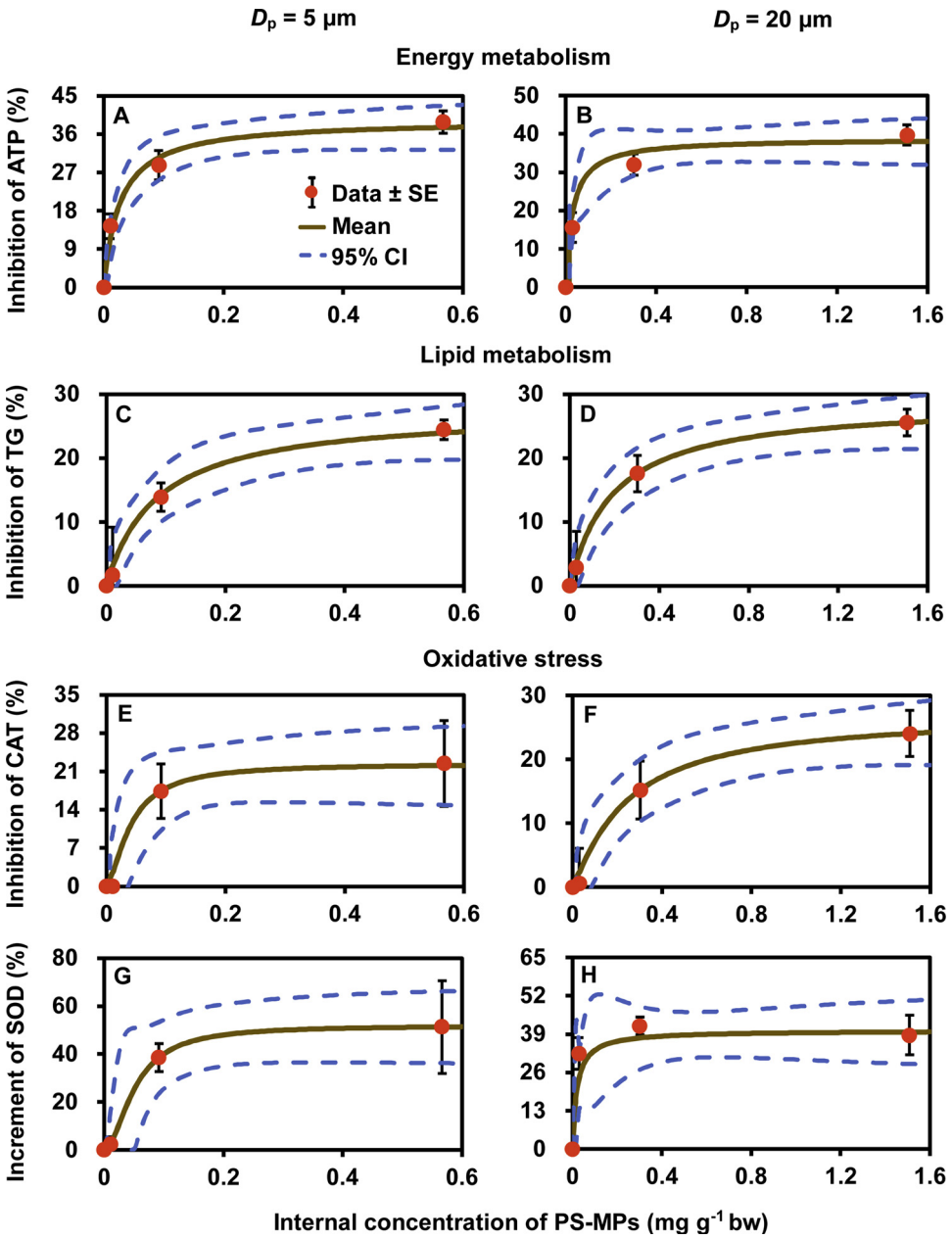

Fig. 4. Optimal fit of the Hill equation model for the relationships between concentrations of 5 and 20 μm PS-MPs and biological markers related to (A, B) energy metabolism, (C, D) lipid metabolism, and (E – H) oxidative stress in the liver of mice.

in this study, it was found that lipid metabolism-associated biomarkers of TG and total cholesterol (TCH) levels in liver tissue were decreased when mice were treated with 1000 μg L^{-1} PS-MP in size of 0.5 or 50 μm [38]. Therefore, in respect of the consistent trends of MPs toxicities in gut, liver, and lipid metabolism in mice system, the employed biomarkers in this study could give a comprehensive overview of potential toxic effects or mechanisms of MPs on specific mice organ that could be optimally (with quantifiable results) applied in the TK/TD and risk assessments.

Notably, similar toxic effects of MPs could be observed in several soil invertebrates based on results of previous studies. Lei et al. [24] observed that PS-MPs significantly enhanced expression of glutathione S-transferase 4 (GST-4), one of the major cellular detoxification enzymes, inducing oxidative stress in Caenorhabditis elegans. A reduction in feeding activity was also observed in lugsworms posed by PS-MPs exposure in concentration of 7.4% dw [33]. It was also revealed that effects of abrasion and obstruction resulted from MPs in digestive tract of worms could lead to dilution and decrements of nutrient bioavailability [33,34] Moreover, Huerta Lwanga et al. [34] indicated that concentrated MPs in casts could cause significant reduction of the survival and tunnel formation of the earthworm *L. terrestris* posed by MPs at concentrations of higher than 28% w/w. Taken together, although the limited evidence of MPs toxicities in mice system, similar and comparable effects of MPs on mice and invertebrates such as activities in respectively digestive system and tract and oxidative stress could be observed, indicating that the biomarkers in PS-MPs-exposed mice applied in this study could be plausibly extrapolated as potential effects to human systems and thus provide a feasible and quantitative methodology for extrapolation approach in future studies.

4.3. Application of mice model to threshold exposure concentrations of MPs in human

In the realm of terrestrial ecosystems, earthworms have been

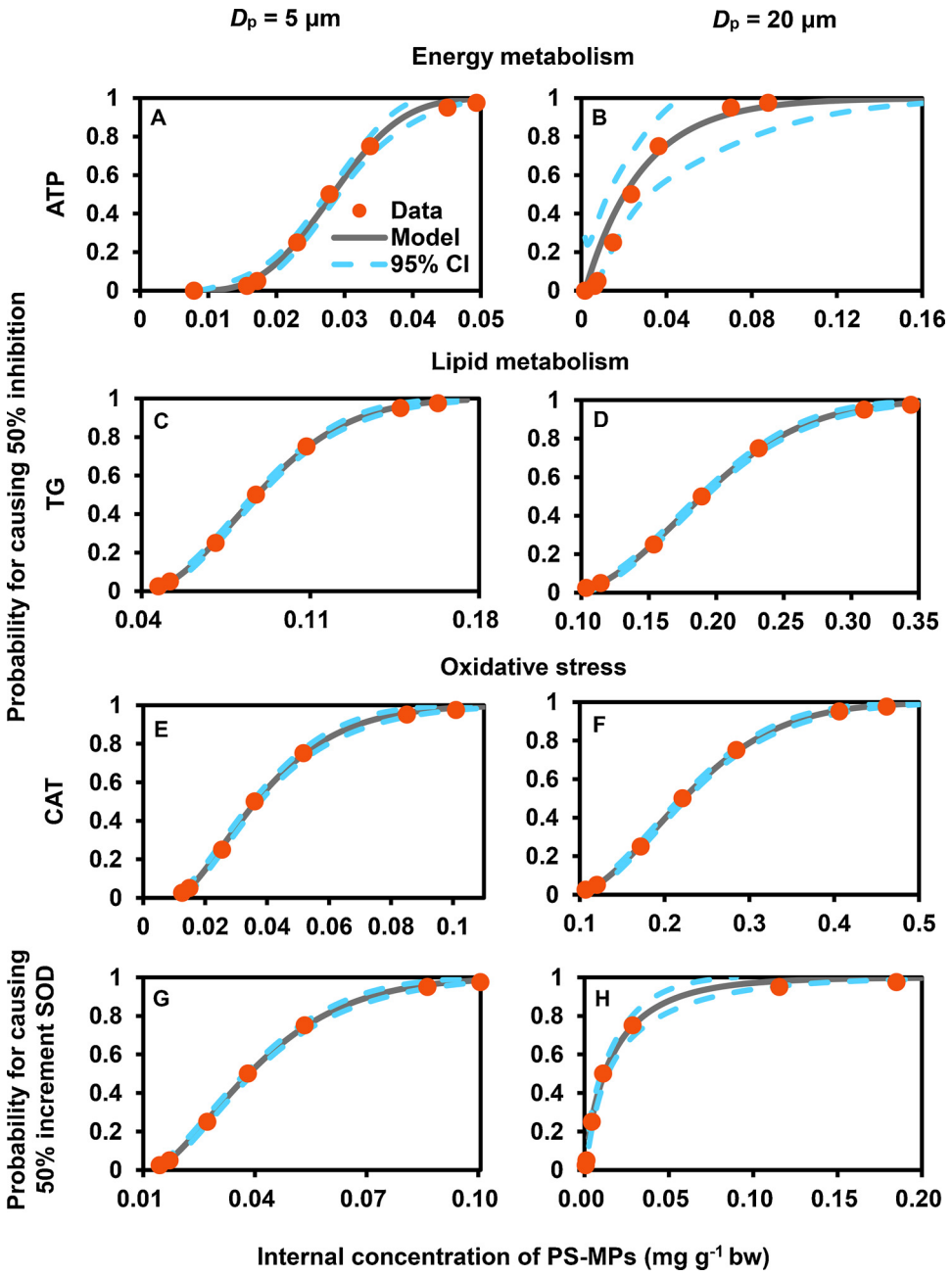

Fig. 5. Best fit of the Weibull threshold model to the cumulative distribution functions of 50% inhibition concentrations of (A, B) ATP, (C, D) TG, (E, F) CAT, and incremental concentration of (G, H) SOD for liver of mice exposed to 5 and 20 μm PS-MPs.

predominantly adopted as a model organism in assessing MPs bioaccumulations in soil species [30]. Deng et al. [21] provided valuable experimental data of PS-MPs bioaccumulation and biomarker responses in mice to benefit the construction of TBTK/TD modeling framework for terrestrial systems in this study. The mouse is the most commonly used animal to model human disease, offering a number of advantages as an animal model since the similarities of physiology and anatomy between mice and humans are matched by substantial genetic homology [40]. Rhomberg and Lewandowski [41] also observed that the concentration-time relationships for mice and humans led to congruity of methotrexate pharmacokinetics, falling to the same concentration after the same amount of physiological time has elapsed, revealing the role of murine system as a robust animal model.

To efficiently evaluate threshold exposure concentrations of MPs in human with limited *in vivo* data in terrestrial organisms, an extrapolation approach from mice to human system based on the integration of rigorous TBTK/TD-based estimations and risk assessment scheme is of urgent need. Several current approaches have provided extrapolation methodologies by multiplying the animal doses at various times to convert doses across species based on body weight and surface area of various species [42]. We have proposed a parsimonious extrapolation algorithm from mice to human systems based on results derived from mechanistic approach constructed in this study. The extrapolated human threshold concentrations of PS-MPs are applicable to risk assessment framework by employing results of TBTK/TD assessment and available environmental concentrations of PS-MPs. It should also be noted that the estimated biokinetic constants are only applicable to interactions between mice and PS-MPs. To obtain threshold levels of PS-MPs in human body extrapolated from those in other species, the proposed extrapolation approach could be adopted based on the developed TBTK/TD modeling framework (if related experimental results are available) and the well-described body weights and allometric

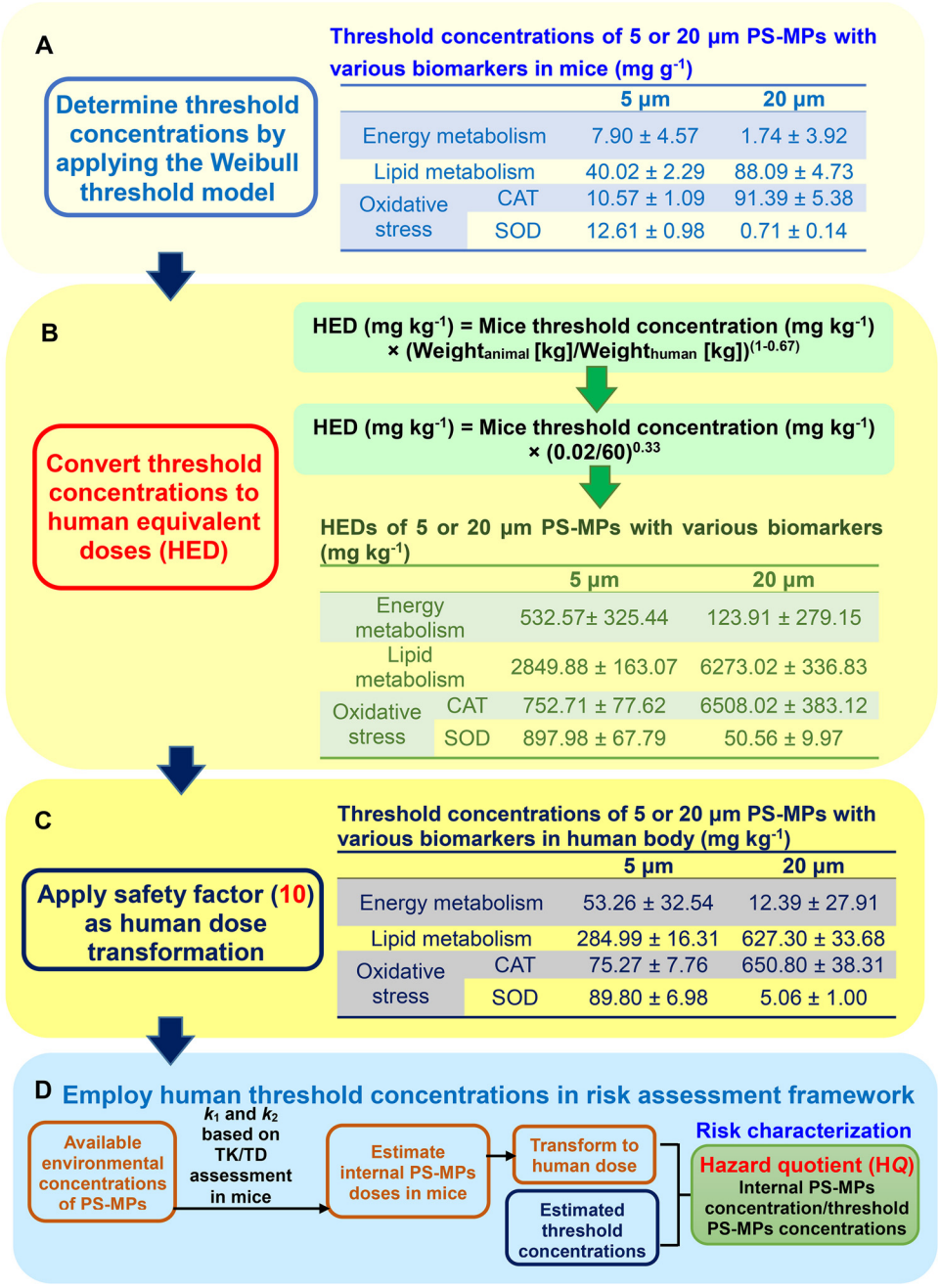

Fig. 6. Schematic illustrating the proposed extrapolation algorithm for extrapolating the results from mice system to humans.

exponents of specific organism.

4.4. Limitations and implications

A broad evidence has demonstrated bioaccumulations of MPs in marine species and trophic transfer effects in food chains of aquatic ecosystem [7,25,43,44]. Miranda and de Carvalho-Souza [45] have indicated that the potency of MPs transferring through food chain were more likely to pose ecological and health-related risks. The bioaccumulation and biomagnification of MPs will flow from lower nutrient levels to higher levels, eventually resulting in human health risks [45,46]. Bouwmeester et al. [47] also suggested that MP sizes ranging from 0.2 to 150 μm, covering the applied PS-MP sizes adopted in this study, can across the gut into lymphatic system in human, indicating that human could potentially accumulate MPs via ingestion.

Due to the large prevalence of MPs floating in surface layer or sinking to sediment, MPs ingestion has been well documented in large pelagic fish that is relevant to human consumption such as bluefin tuna (12.1%), albacore (9.7%), and swordfish (4.2%) as well as in demersal fish (32.34%) from the English Channel [14,48]. Wright and Kelly [49] also revealed that MPs can accumulate and exert dose-dependent localized-particle toxicity by inducing inflammation and immune mechanisms in human, implying that the dose-response relationship between MPs concentrations and biological effects can be furtherly applied to human health assessment for chronic exposures of MPs.

Scientists can use animal studies to study the TK and TD aspects of environmental toxicants, and the estimated threshold exposures or maximum permissible exposures can be interpreted for determining human risk [28,50]. However, it should be noted that the exposure dose of 0.01 mg PS-MPs day^{-1} (~10^5 particles for 5 μm and ~10^3 for 20 μm) in this study [21], was higher than the daily dosage (~30 particles day^{-1}) of MPs consumption of European shellfish, indicating

that the estimated threshold dose could be appropriately modified in populations posed by different MPs concentrations [15]. Furthermore, both ingestion and inhalation were reported to be exposure pathways of MPs, the TBTK/TD assessment could be essentially strengthened when experimental data of MPs exposures via inhalation route in mammalian system are available [49].

5. Conclusions

The TBTK/TD modeling framework has evaluated organ-specific biokinetic constants in which the highest average BCF_{ss} for 5 and 20 μm MPs treatments were 8.16 and 4.66 in mice liver, respectively. Threshold concentration estimates of 5 and 20 μm MPs for the most sensitive biomarkers in mice were correspondingly 7.90 ± 4.57 and 0.71 ± 0.14 μg g^{-1} bw. We also estimated that human threshold concentrations of 5 and 20 μm MPs were 53.26 ± 32.54 and 5.06 ± 1 mg g^{-1} for the most sensitive biomarkers, respectively, based on the extrapolation algorithm. We conclude that application of the TBTK/TD model scheme by utilizing mice system could effectively facilitate the progress of MPs risk assessment in light of the limited knowledge in MPs research in human health. We suggest that results derived from TBTK/TD assessment, Weibull threshold model, and the extrapolation algorithm could be adopted to rapidly evaluate MPs-induced toxicities at various concentrations and sizes and offer a mechanistic tool in human health risk assessment scheme.

Conflicts of interest

The authors declare that no competing interests exist.

Acknowledgement

This study was supported by the Ministry of Science and Technology of the Republic of China under Grant MOST 105-2313-B-002-020-MY3.

Appendix A. Supplementary data

Supplementary material related to this article can be found, in the online version, at doi:https://doi.org/10.1016/j.jhazmat.2018.12.048.

References

[1] A.L. Andrady, Microplastics in the marine environment, Mar. Pollut. Bull. 62 (2011) 1596–1605, https://doi.org/10.1016/j.marpolbul.2011.05.030.
[2] M. Cole, P. Lindeque, E. Fileman, C. Halsband, R. Goodhead, J. Moger, T.S. Galloway, Microplastic ingestion by zooplankton, Environ. Sci. Technol. 47 (2013) 6646–6655, https://doi.org/10.1021/es400663f.
[3] C.J. Moore, Synthetic polymers in the marine environment: a rapidly increasing, long-term threat, Environ. Res. 108 (2008) 131–139, https://doi.org/10.1016/j.envres.2008.07.025.
[4] T.J. Suhrhoff, B.M. Scholz-Böttcher, Qualitative impact of salinity, UV radiation and turbulence on leaching of organic plastic additives from four common plastics—a lab experiment, Mar. Pollut. Bull. 102 (2016) 84–94, https://doi.org/10.1016/j.marpolbul.2015.11.054.
[5] A. Katsnelson, News feature: microplastics present pollution puzzle, Proc. Natl. Acad. Sci. 112 (2015) 5547–5549, https://doi.org/10.1073/pnas.1504135112.
[6] C.M. Rochman, M.A. Browne, B.S. Halpern, B.T. Hentschel, E. Hoh, H.K. Karapanagioti, L.M. Rios-Mendoza, H. Takada, S. Teh, R.C. Thompson, Policy: classify plastic waste as hazardous, Nature 494 (2013) 169, https://doi.org/10.1038/494169a.
[7] M.A. Browne, A. Dissanayake, T.S. Galloway, D.M. Lowe, R.C. Thompson, Ingested microscopic plastic translocates to the circulatory system of the mussel, *Mytilus edulis* (L.), Environ. Sci. Technol. 42 (2008) 5026–5031, https://doi.org/10.1021/es800249a.
[8] C.G. Avio, S. Gorbi, F. Regoli, Experimental development of a new protocol for extraction and characterization of microplastics in fish tissues: first observations in commercial species from Adriatic Sea, Mar. Environ. Res. 111 (2015) 18–26, https://doi.org/10.1016/j.marenvres.2015.06.014.
[9] B. De Witte, L. Devriese, K. Bekaert, S. Hoffman, G. Vandermeersch, K. Cooreman, J. Robbens, Quality assessment of the blue mussel (*Mytilus edulis*): comparison between commercial and wild types, Mar. Pollut. Bull. 85 (2014) 146–155, https://doi.org/10.1016/j.marpolbul.2014.06.006.
[10] E.M. Foekema, C. De Gruijter, M.T. Mergia, J.A. van Franeker, A.J. Murk, A.A. Koelmans, Plastic in north sea fish, Environ. Sci. Technol. 47 (2013) 8818–8824, https://doi.org/10.1021/es400931b.
[11] J. Li, D. Yang, L. Li, K. Jabeen, H. Shi, Microplastics in commercial bivalves from China, Environ. Pollut. 207 (2015) 190–195, https://doi.org/10.1016/j.envpol.2015.09.018.
[12] G. Liebezeit, E. Liebezeit, Non-pollen particulates in honey and sugar, Food Addit. Contam. A 30 (2013) 2136–2140, https://doi.org/10.1080/19440049.2013.843025.
[13] G. Liebezeit, E. Liebezeit, Synthetic particles as contaminants in German beers, Food Addit. Contam. A 31 (2014) 1574–1578, https://doi.org/10.1080/19440049.2014.945099.
[14] T. Romeo, B. Pietro, C. Pedà, P. Consoli, F. Andaloro, M.C. Fossi, First evidence of presence of plastic debris in stomach of large pelagic fish in the Mediterranean Sea, Mar. Pollut. Bull. 95 (2015) 358–361, https://doi.org/10.1016/j.marpolbul.2015.04.048.
[15] L. Van Cauwenberghe, C.R. Janssen, Microplastics in bivalves cultured for human consumption, Environ. Pollut. 193 (2014) 65–70, https://doi.org/10.1016/j.envpol.2014.06.010.
[16] B.E. Oßmann, G. Sarau, H. Holtmannspötter, M. Pischetsrieder, S.H. Christiansen, W. Dicke, Small-sized microplastics and pigmented particles in bottled mineral water, Water Res. 141 (2018) 307–316, https://doi.org/10.1016/j.watres.2018.05.027.
[17] S.A. Mason, V. Welch, J. Neratko, Synthetic Polymer Contamination in Bottled Water, Department of Geology and Environmental Sciences, Fredonia University, New York, 2018 Available from: (Accessed 23 March 2018) http://news.bbc.co.uk/2/shared/bsp/hi/pdfs/14_03_13_finalbottled.pdf.
[18] R. Ashauer, B.I. Escher, Advantages of toxicokinetic and toxicodynamic modelling in aquatic ecotoxicology and risk assessment, J. Environ. Monit. 12 (2010) 2056–2061, https://doi.org/10.1039/C0EM00234H.
[19] B.Y.H. Chou, C.M. Liao, M.C. Lin, H.H. Cheng, Toxicokinetics/toxicodynamics of arsenic for farmed juvenile milkfish *Chanos chanos* and human consumption risk in BFD-endemic area of Taiwan, Environ. Int. 32 (2006) 545–553, https://doi.org/10.1016/j.envint.2006.01.004.
[20] J.W. Tsai, W.Y. Chen, Y.R. Ju, C.M. Liao, Bioavailability links mode of action can improve the long-term field risk assessment for tilapia exposed to arsenic, Environ. Int. 35 (2009) 727–736, https://doi.org/10.1016/j.envint.2009.01.014.
[21] Y. Deng, Y. Zhang, B. Lemos, H. Ren, Tissue accumulation of microplastics in mice and biomarker responses suggest widespread health risks of exposure, Sci. Rep. 7 (2017) 46687, https://doi.org/10.1038/srep46687.
[22] F. Faure, C. Demars, O. Wieser, M. Kunz, L.F. De Alencastro, Plastic pollution in Swiss surface waters: nature and concentrations, interaction with pollutants, Environ. Chem. 12 (2015) 582–591, https://doi.org/10.1071/EN14218.
[23] M. Di, J. Wang, Microplastics in surface waters and sediments of the Three Gorges Reservoir, China, Sci. Total Environ. 616 (2018) 1620–1627, https://doi.org/10.1016/j.scitotenv.2017.10.150.
[24] L. Lei, M. Liu, Y. Song, S. Lu, J. Hu, C. Cao, B. Xie, H. Shi, D. He, Polystyrene (nano) microplastics cause size-dependent neurotoxicity, oxidative damages and other adverse effects in Caenorhabditis elegans, Environ. Sci. Nano 5 (2018) 2009–2020, https://doi.org/10.1039/C8EN00412A.
[25] P. Farrell, K. Nelson, Trophic lvel transfer of microplastic:*Mytilus edulis* (L.) to *Carcinus maenas* (L.), Environ. Pollut. 177 (2013) 1–3, https://doi.org/10.1016/j.envpol.2013.01.046.
[26] US Food and Drug Administration, Guidance for Industry: Estimating the Maximum Safe Starting Dose in Initial Clinical Trials for Therapeutics in Adult Healthy Volunteers, Center for Drug Evaluation and Research (CDER), 2005 (Accessed 20 November 2018, http://www.fda.gov/downloads/Drugs/Guidances/UCM078932.pdf.
[27] J.W. Shin, I.C. Seol, C.G. Son, Interpretation of animal dose and human equivalent dose for drug development, J. Korean Orient. Med. 31 (2010) 1–7.
[28] A.B. Nair, S. Jacob, A simple practice guide for dose conversion between animals and human, J. Basic Clin. Pharm. 7 (2016) 27, https://doi.org/10.4103/0976-0105.177703.
[29] B.G. Reigner, K.S. Blesch, Estimating the starting dose for entry into humans: principles and practice, Eur. J. Clin. Pharmacol. 57 (2002) 835–845, https://doi.org/10.1007/s00228-001-0405-6.
[30] Y. Chae, Y.J. An, Current research trends on plastic pollution and ecological impacts on the soil ecosystem: a review, Environ. Pollut. 240 (2018) 387–395, https://doi.org/10.1016/j.envpol.2018.05.008.
[31] M.C. Rillig, Microplastic in terrestrial ecosystems and the soil? Environ. Sci. Technol. 46 (2012) 6453–6454, https://doi.org/10.1021/es302011r.
[32] M. Liu, S. Lu, Y. Song, L. Lei, J. Hu, W. Lv, W. Zhou, C. Cao, H. Shi, X. Yang, D. He, Microplastic and mesoplastic pollution in farmland soils in suburbs of Shanghai, China, Environ. Pollut. 242 (2018) 855–862, https://doi.org/10.1016/j.envpol.2018.07.051.
[33] E. Besseling, A. Wegner, E.M. Foekema, M.J. van den Heuvel-Greve, A.A. Koelmans, Effects of microplastic on fitness and PCB bioaccumulation by the lugworm *Arenicola marina* (L.), Environ. Sci. Technol. 47 (2013) 593–600, https://doi.org/10.1021/es302763x.
[34] E. Huerta Lwanga, H. Gertsen, H. Gooren, P. Peters, T. Salánki, M. van der Ploeg, E. Besseling, A.A. Koelmans, V. Geissen, Microplastics in the terrestrial ecosystem: implications for *Lumbricus terrestris* (Oligochaeta, Lumbricidae), Environ. Sci. Technol. 50 (2016) 2685–2691, https://doi.org/10.1021/acs.est.5b05478.
[35] B.L. Tang, Commentary: Tissue accumulation of microplastics in mice and biomarker responses suggest widespread health risks of exposure, Front. Environ. Sci. 5 (2017) 63, https://doi.org/10.3389/fenvs.2017.00063.
[36] E. Huerta Lwanga, J. Mendoza Vega, V. Ku Quej, J.L.A. Chi, L. Sanchez Del Cid,

C. Chi, G. Escalona Segura, H. Gertsen, T. Salánki, M. van der Ploeg, A.A. Koelmans, V. Geissen, Field evidence for transfer of plastic debris along a terrestrial food chain, Sci. Rep. 7 (2017) 14071, https://doi.org/10.1038/s41598-017-14588-2.
[37] S. Zhao, L. Zhu, D. Li, Microscopic anthropogenic litter in terrestrial birds from Shanghai, China: not only plastics but also natural fibers, Sci. Total Environ. 550 (2016) 1110–1115, https://doi.org/10.1016/j.scitotenv.2016.01.112.
[38] L. Lu, Z. Wan, T. Luo, Z. Fu, Y. Jin, Polystyrene microplastics induce gut microbiota dysbiosis and hepatic lipid metabolism disorder in mice, Sci. Total Environ. 631 (2018) 449–458, https://doi.org/10.1016/j.scitotenv.2018.03.051.
[39] Y. Jin, L. Lu, W. Tu, T. Luo, Z. Fu, Impacts of polystyrene microplastic on the gut barrier, microbiota and metabolism of mice, Sci. Total Environ. 649 (2019) 308–317, https://doi.org/10.1016/j.scitotenv.2018.08.353.
[40] E.W. Uhl, N.J. Warner, Mouse models as predictors of human responses: evolutionary medicine, Curr. Pathobiol. Rep. 3 (2015) 219–223, https://doi.org/10.1007/s40139-015-0086-y.
[41] L.R. Rhomberg, T.A. Lewandowski, Methods for identifying a default cross-species scaling factor, Hum. Ecol. Risk Assess. 12 (2006) 1094–1127, https://doi.org/10.1080/10807030600977269.
[42] US EPA, Recommended Use of Body Weight$^{3/4}$ as the Default Method in Derivation of the Oral Reference Dose, Office of the Science Advisor, Risk Assessment Forum, US Environmental Protection Agency, Washington DC, 2011 (Accessed 6 August 2018, https://www.epa.gov/risk/recommended-use-body-weight-34-default-method-derivation-oral-reference-dose.
[43] M. Cole, P. Lindeque, C. Halsband, T.S. Galloway, Microplastics as contaminants in the marine environment: a review, Mar. Pollut. Bull. 62 (2011) 2588–2597, https://doi.org/10.1016/j.marpolbul.2011.09.025.
[44] C.M. Rochman, T. Kurobe, I. Flores, S.J. Teh, Early warning signs of endocrine disruption in adult fish from the ingestion of polyethylene with and without sorbed chemical pollutants from the marine environment, Sci. Total Environ. 493 (2014) 656–661, https://doi.org/10.1016/j.scitotenv.2014.06.051.
[45] D.D.A. Miranda, G.F. de Carvalho-Souza, Are we eating plastic-ingesting fish? Mar. Pollut. Bull. 103 (2016) 109–114, https://doi.org/10.1016/j.marpolbul.2015.12.035.
[46] N. Seltenrich, New link in the food chain? Marine plastic pollution and seafood safety, Environ. Health Perspect. 123 (2015) A34–A41, https://doi.org/10.1289/ehp.123-A34.
[47] H. Bouwmeester, P.C.H. Hollman, R.J.B. Peters, Potential health impact of environmentally released micro- and nanoplastics in the human food production chain: experiences from nanotoxicology, Environ. Sci. Technol. 49 (2015) 8932–8947, https://doi.org/10.1021/acs.est.5b01090.
[48] A.L. Lusher, M. McHugh, R.C. Thompson, Occurrence of microplastics in the gastrointestinal tract of pelagic and demersal fish from the English Channel, Mar. Pollut. Bull. 67 (2013) 94–99, https://doi.org/10.1016/j.marpolbul.2012.11.028.
[49] S.L. Wright, F.J. Kelly, Plastic and human health: A micro issue? Environ. Sci. Technol. 54 (2017) 6634–6647, https://doi.org/10.1021/acs.est.7b00423.
[50] R.L. Brent, Utilization of animal studies to determine the effects and human risks of environmental toxicants (drugs, chemicals, and physical agents), Pediatrics 113 (Suppl. 3) (2004) 984–995.